# Supplementary Information for

## Interface Phase Engineering of Monolayer $Sb_2O_3$ on Au (111)

Jiyuan Zhang,[ab] Haoyu Zhao,[*b] Shuning Cai,[b] Xueqing Yang,[b] Yabin Zhang,[b] Bingkai Yuan,[b] Junyong Wang,[b] Jingzhe Chen,[a] Pengru Huang,[*c] and Gaolei Zhan[*b]

[a] Department of Physics, College of Sciences, Shanghai University, Shanghai 200444, P.R. China.

[b] Suzhou Institute of Nano-Tech and Nano-Bionics of the Chinese Academy of Sciences, 398 Ruoshui Road, Suzhou, Jiangsu, 215123, P. R. China.

[c] Institute for Functional Intelligent Materials (I-FIM), National University of Singapore, Singapore 117544, Singapore.

[d] Guangdong Institute of Semiconductor Micro-Nano Manufacturing Technology, Foshan 528225, P.R. China.

## Methods

### STM measurements

All experiments were performed in a commercial ultra-high-vacuum (UHV) variable-temperature scanning probe microscope (VT-STM, Scienta Omicron) operated with an Omicron control system. A homemade K-cell evaporator was integrated into the UHV chamber for molecular deposition. Prior to use, the Au (111) (Phasis, Switzerland) surfaces were cleaned by repeated cycles of $Ar^+$ sputtering followed by thermal annealing. Antimony trioxide molecules (Aladdin,99.999%) were thermally evaporated onto Au (111) substrates held at temperatures ranging from 298 K to 473 K. STM measurements were carried out at 300 K in constant-current mode. The tunneling bias voltages were applied to the sample (denoted as $V_s$), and the tunneling current is indicated as $I_t$ in the figure captions. STM images were processed using the Scanning Probe Image Processor (SPIP, Image Metrology ApS).

### Computational Methods

Our calculations are based on density functional theory (DFT) using the PBE functional as implemented in the Vienna Ab Initio Simulation Package (VASP).[1, 2] The interaction between the valence electrons and ionic cores is described within the projector augmented (PAW) approach with a plane-wave energy cutoff of 500 eV.[3] The DFT-D3 method with the Becke-Johnson damping function was included to describe the dispersive inter cluster interactions of inorganic molecular crystals.[4] The Brillouin zone was sampled by Monkhorst−Pack mesh s of $0.03*2\pi$ $Å^{-1}$.To avoid spurious interactions between periodic images, a vacuum spacing of approximately 15 Å was introduced along the non-periodic direction. Considering the large number of atoms involved, the Au(111) surface was modeled using a three-layer slab to investigate the substrate–adsorbate interactions. In the structural energy minimization, the atomic coordinates are allowed to relax until the forces on all the atoms are less than 0.01 eV/Å. The energy tolerance is $10^{-6}$ eV. The dielectric tensors originated from electronic and ionic contributions were calculated by using density functional perturbation (DFPT) and the finite difference approach respectively.

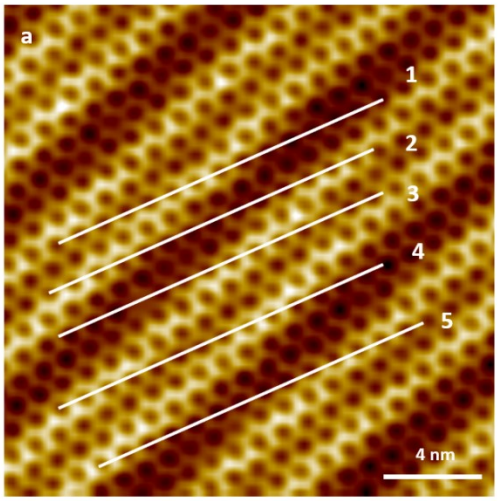


| Line | 1 | 2 | 3 | 4 | 5 |
|---|---|---|---|---|---|
| Distance across 11 pores (nm) | 10.48 | 10.48 | 10.30 | 10.48 | 10.48 |
| Average spacing between two adjacent pores (nm) | 1.048 | 1.048 | 1.03 | 1.048 | 1.048 |
| Mean pore–pore distance (nm) | 1.044 | | | | |

**Figure. S1** (a) STM image of the hexagonal porous phase. Five representative line profiles were extracted across the pores to quantify the pore–pore distances, and the measured values are summarized in the table. Set point: $V_s$ = -2 V, $I_t$ = 10 pA.

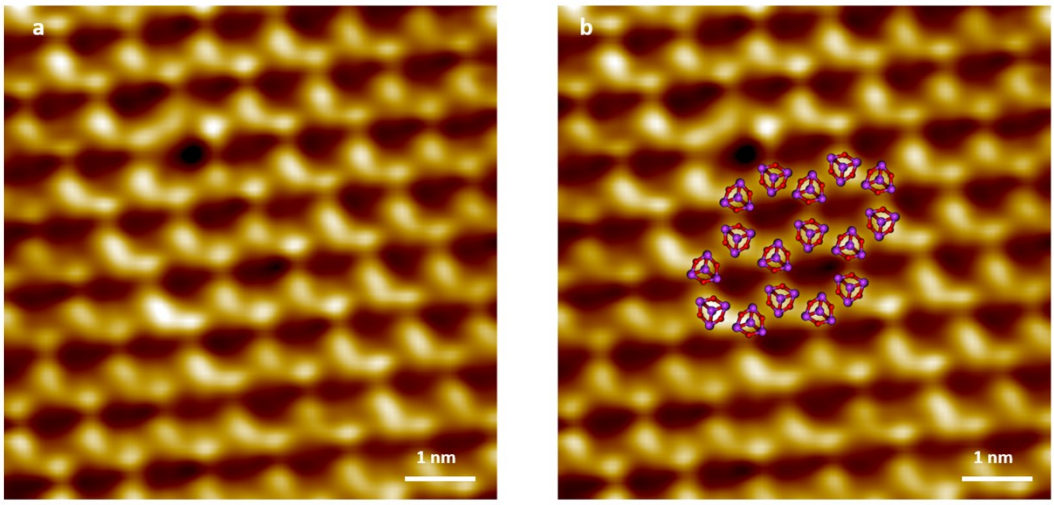


**Figure. S2** High-resolution STM image of phase **1.** (a) Original STM image and (b) the same image superimposed with a structural model (b). Set point: $V_s$ = -2V, $I_t$ =10 pA.

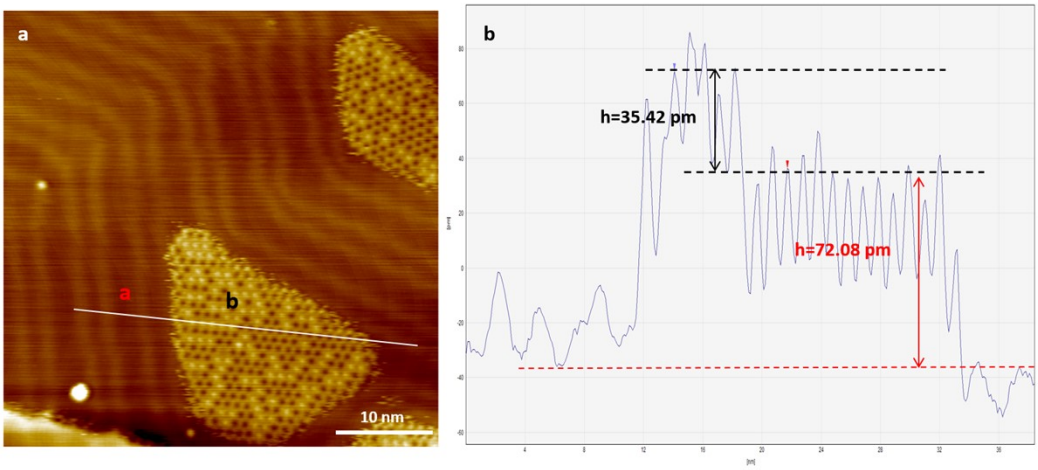


**Figure. S3** (a) STM image show that hexagonal porous phase emerged simultaneously with the hexagonal close-packed phase during epitaxial growth. Set point: $V_s$ = −2 V, $I_t$ = 10 pA. (b) STM height profile along the white line highlighted in (a) shows the apparent height difference between porous hexagonal phase and bare Au substrate is 72 pm and the apparent height difference between brighter spots and surrounded darker spots of the close-packed hexagonal phase is 35 pm.

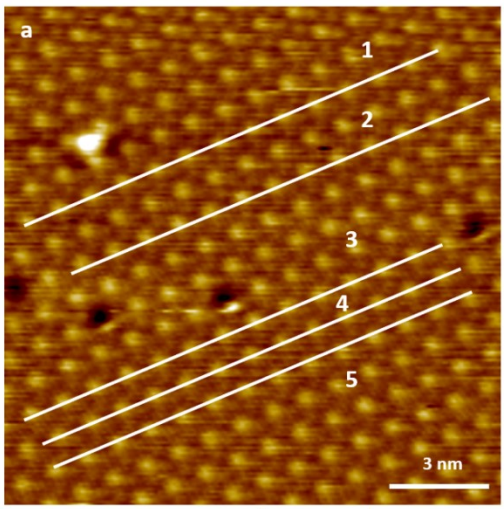


| Line | 1 | 2 | 3 | 4 | 5 |
|---|---|---|---|---|---|
| Distance across 11 pores (nm) | 10.50 | 10.37 | 10.45 | 10.45 | 10.45 |
| Average spacing between two adjacent pores (nm) | 1.05 | 1.037 | 1.045 | 1.045 | 1.045 |
| Mean pore–pore distance (nm) | 1.044 | | | | |

**Figure. S4** (a) STM image of the hexagonal close-packed phase. Five representative line profiles were extracted across the pores to quantify the pore–pore distances, and the measured values are summarized in the table. Set point: $V_s$ = -2 V, $I_t$ = 10 pA.

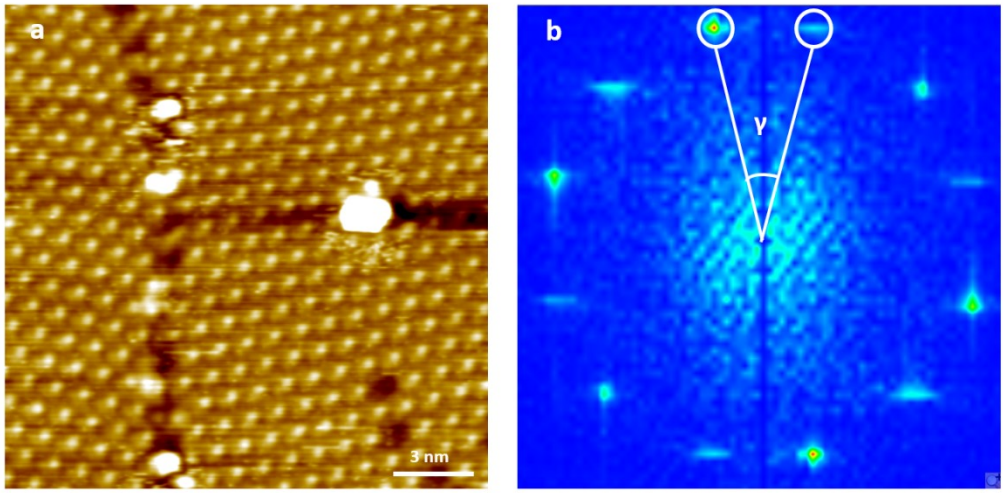


**Figure. S5** (a) STM image of the close-packed phase showing two domains with two distinct orientations. Set point: $V_s$ = −2 V, $I_t$ = 10 pA. (b) Fast Fourier transform (FFT) analysis of image (a) shows that the angle between the two orientations is 28°.

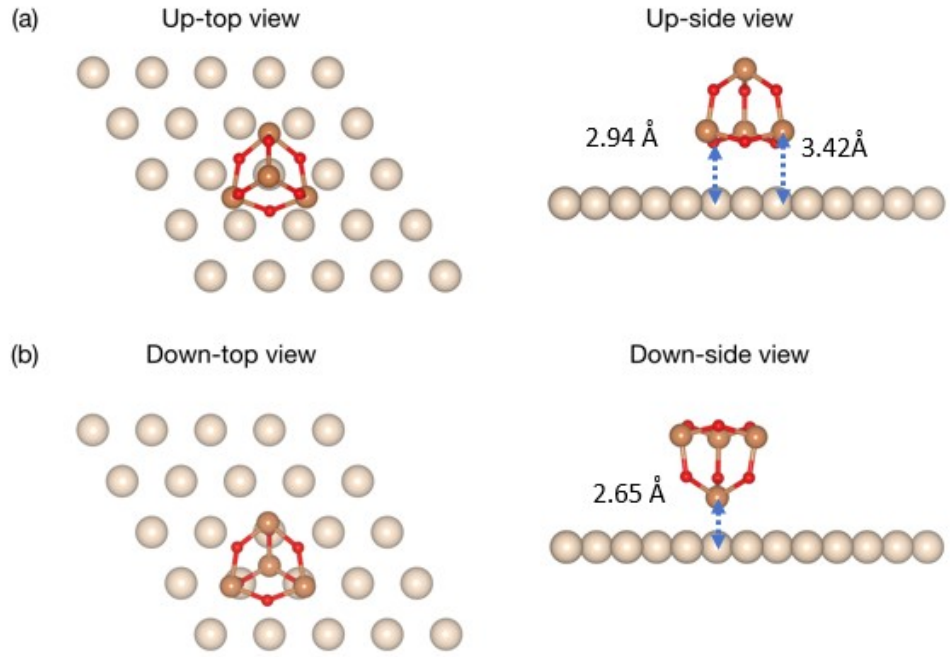


**Figure. S6** The adsorption geometries of Sb4O6 on Au (111) with the upward(a) and downward(b) molecule orientations respectively. For the downward adsorption configuration, the lowest Sb atom is positioned directly above a threefold hollow site, with an adsorption height of 2.65 Å. In contrast, for the upward adsorption configuration, due to size mismatch effects, the three lowest Sb atoms are slightly displaced from the hollow sites toward the bridge sites. In this case, the Sb–Au heights are approximately 3.42 Å, while the O–Au heights are about 2.94 Å. The adsorption energies for the upward and downward configurations are calculated to be -0.74 eV and -0.86 eV per molecule, respectively. Accordingly, the energy cost required to switch the adsorption mode from the upward to the downward configuration is approximately 0.12 eV. This energy difference should be attributed to dipole effects as well as the closer proximity of the molecule to the Au surface in the downward configuration.

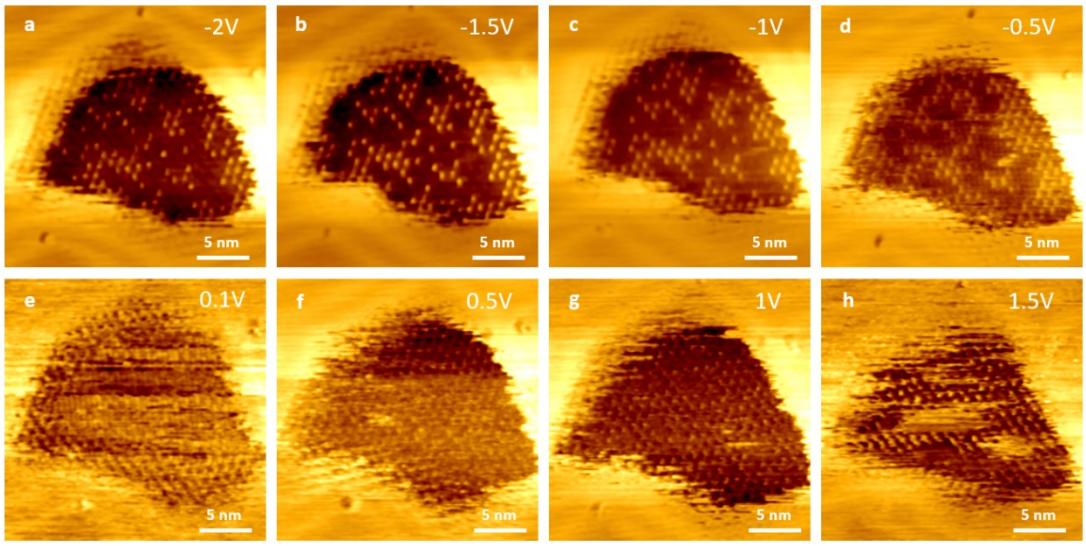


**Figure. S7** (a)–(h) STM images acquired from the same scanning region with different sample biases ranging from -2 V to 1.5 V. Imaging conditions: $I_t$ = 10 pA.

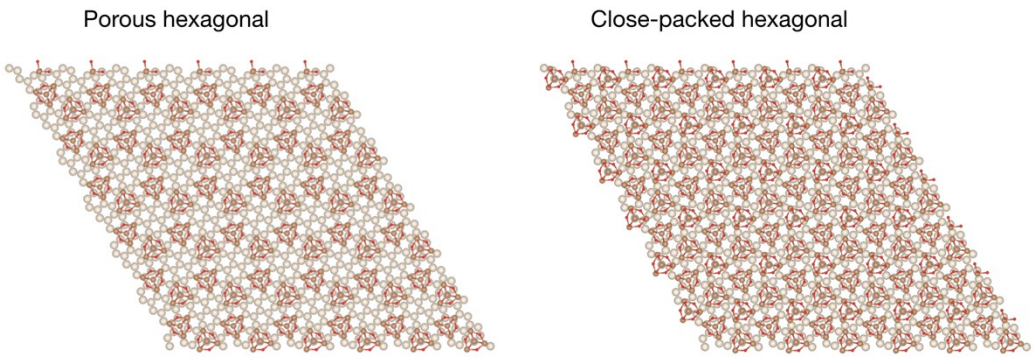


**Figure. S8** The DFT-relaxed structures of the phases on Au (111). The adsorption energies of phase 1 and phase 1’ on Au(111) have been calculated to compare their relative stability, yielding values of −0.94 eV and −0.89 eV per molecule, respectively.

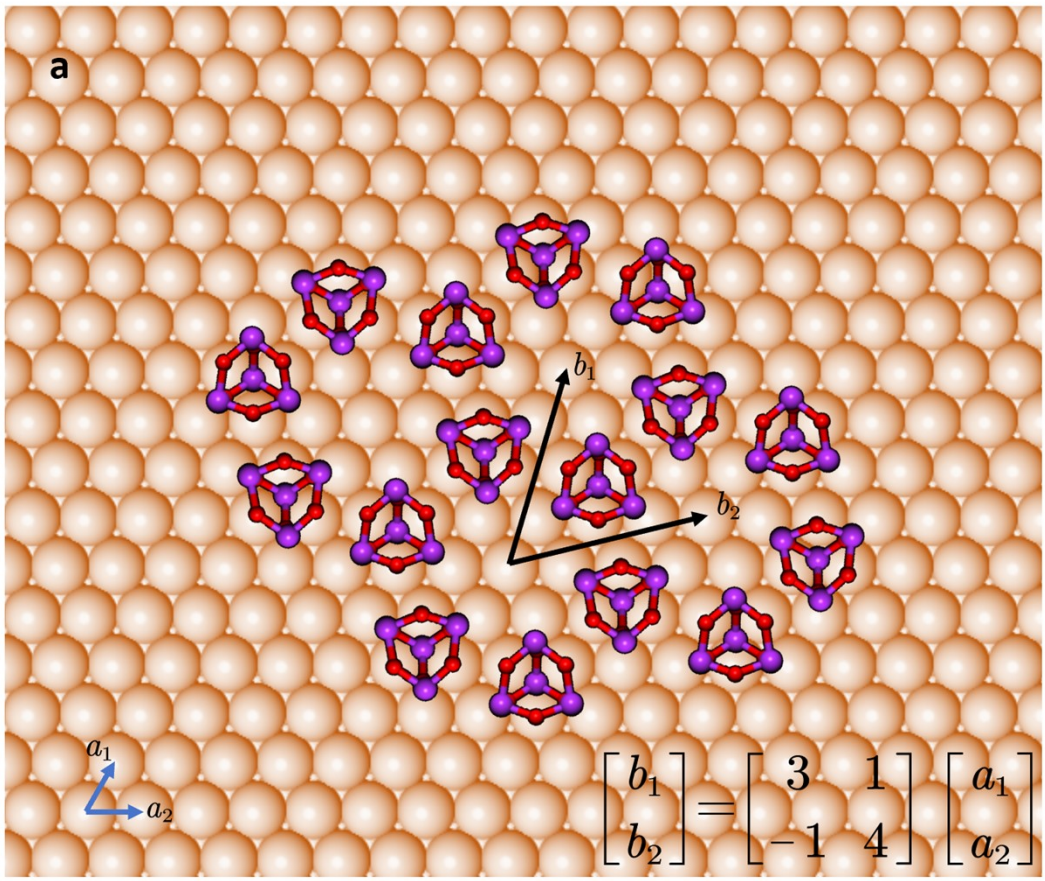


**Figure. S9** (a) The epitaxial relationship between Au(111) lattice and molecular lattice. $|b_1|=|b_2|=1.05$ nm

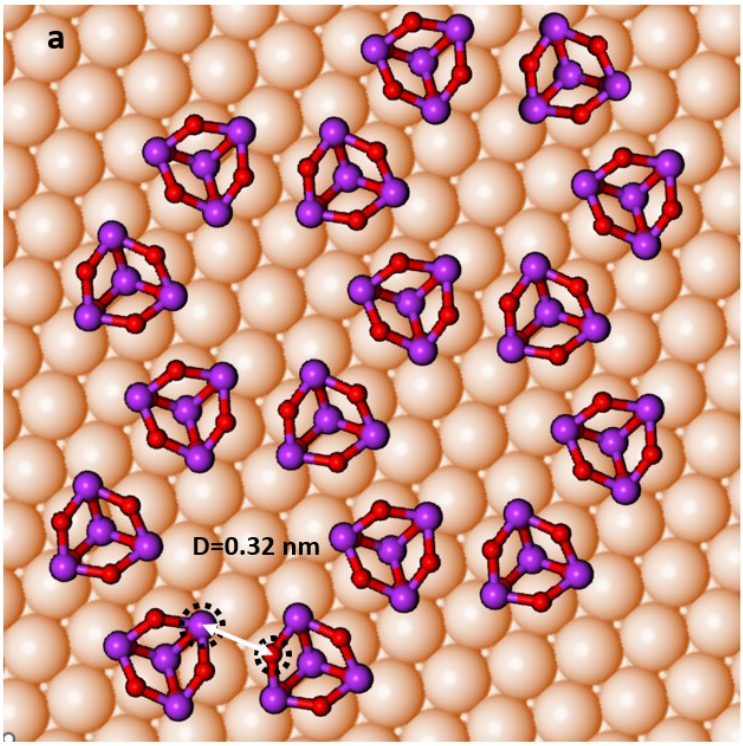


**Figure S10.** (a) The intermolecular distances of two adjacent $Sb_4O_6$ molecules is measured to be 0.32 nm between Sb and O atoms.

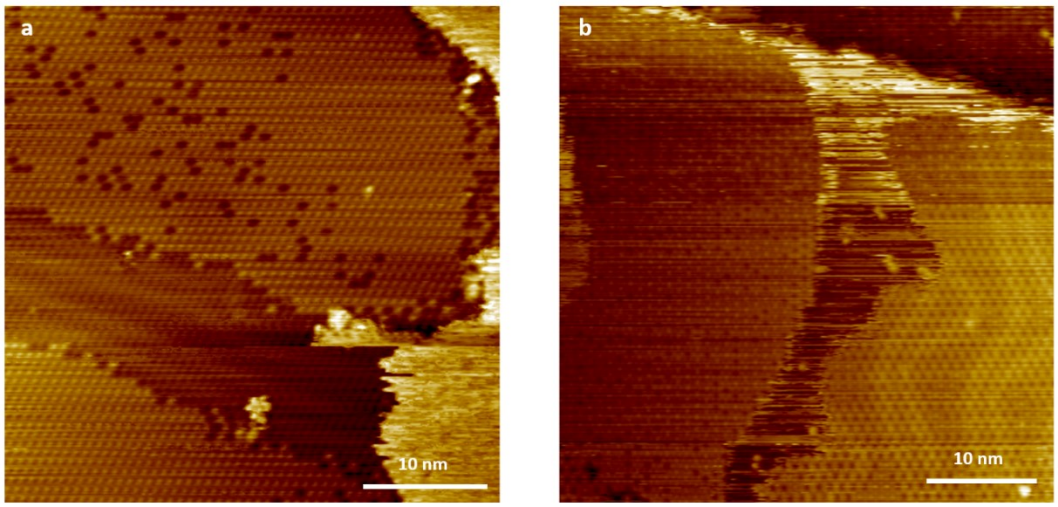


**Figure. S11** (a, b) Representative STM images showing that the herringbone reconstruction of the Au (111) substrate was observed in the porous phase, whereas in close-packed hexagonal, herringbone feature feature is not visible. Set point: (a and b) $V_s$ = -2 V, $I_t$ = 10 pA.

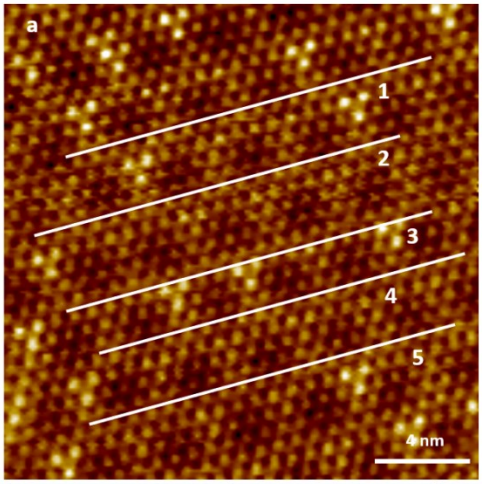


| Line | 1 | 2 | 3 | 4 | 5 |
|---|---|---|---|---|---|
| Distance across 11 pores (nm) | 7.91 | 8.03 | 8.03 | 8.15 | 7.91 |
| Average spacing between two adjacent pores (nm) | 0.791 | 0.803 | 0.803 | 0.815 | 0.791 |
| Mean pore–pore distance (nm) | 0.80 | | | | |

**Figure. S12** (a) STM image of the **α** phase. Five representative line profiles were extracted across the pores to quantify the pore–pore distances, and the corresponding values are summarized in the table. Set point: $V_s$ = -2 V, $I_t$ = 10 pA.

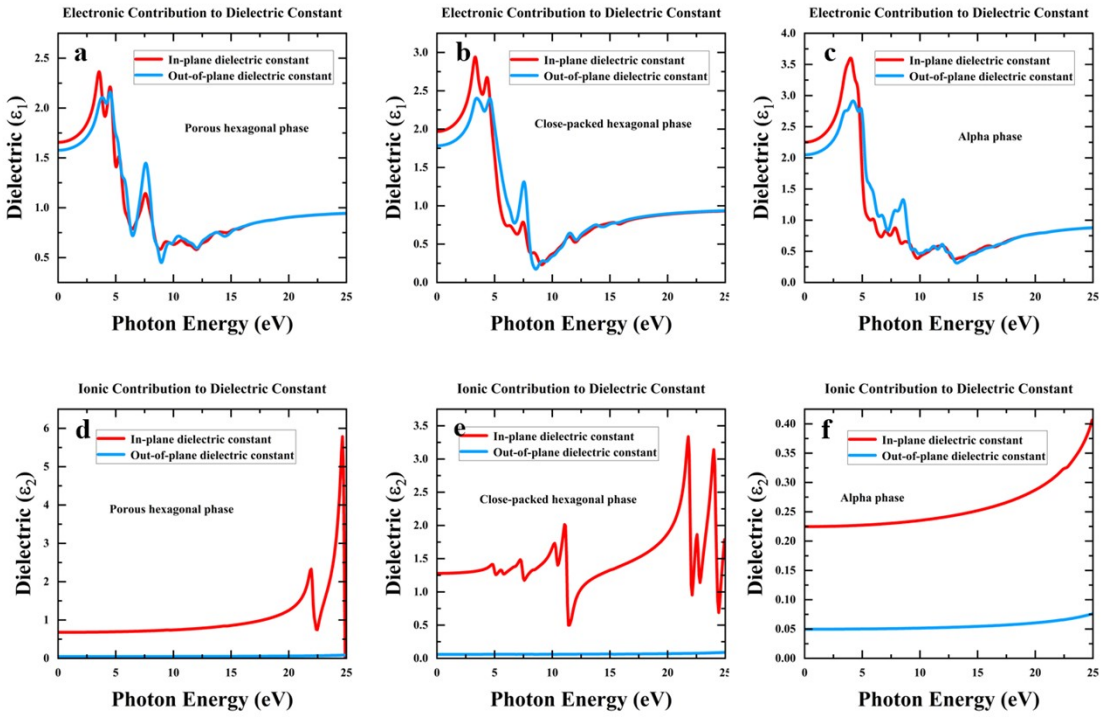


**Figure. S13** Frequency-dependent dielectric response of different $Sb_2O_3$ phases on Au(111). (a–c) Electronic contribution ($\varepsilon_1$) to the dielectric constant as a function of photon energy for the porous hexagonal phase (a), close-packed hexagonal phase (b), and α phase (c). (d–f) Ionic contribution ($\varepsilon_2$) to the dielectric constant for the corresponding porous hexagonal phase (d), close-packed hexagonal phase (e), and α phase (f). Red and blue curves represent the in-plane and out-of-plane components, respectively.

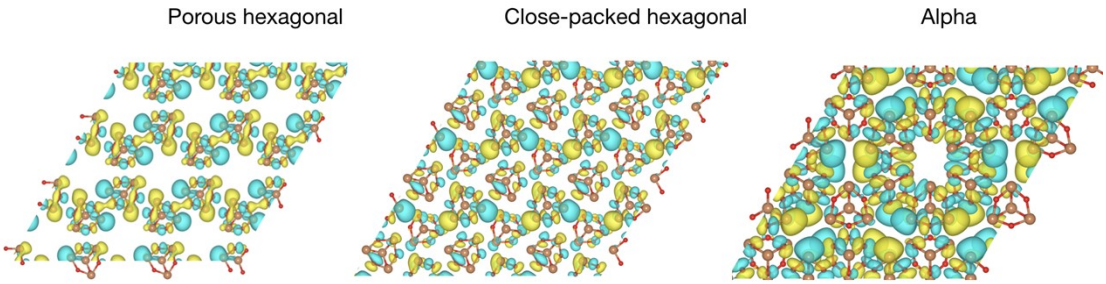


**Figure. S14**. Γ-point wavefunction isosurfaces of the HOMO for the three phases.

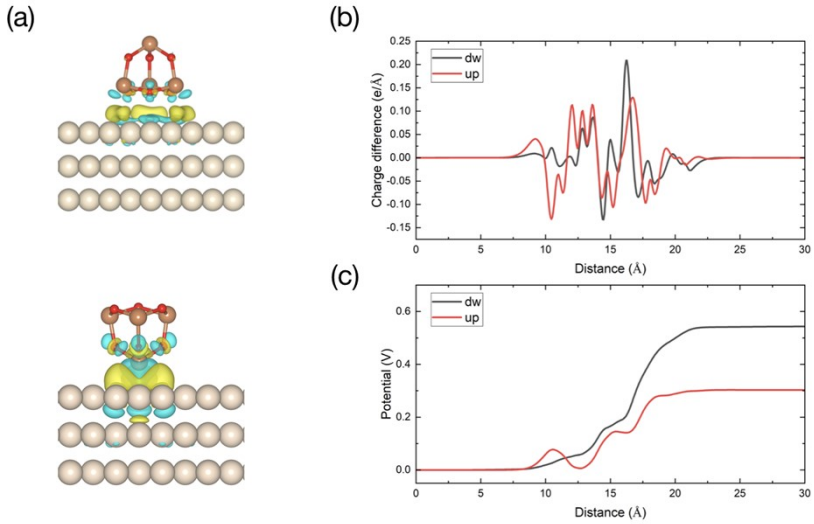


(d)

| Atom | Phase 1 | Phase 1’ | Alpha |
|---|---|---|---|
| Sb | -1.40 | -1.42 | 1.41 |
| O | 0.94 | 0.95 | 0.94 |

**Figure. S15**. Charge transfer for the adsorption structures of $Sb_4O_6$ on Au(111) in the upward and downward configurations. (a) Three-dimensional isosurface plots of the charge density difference; (b) planar-averaged charge density difference along the surface normal; and (c) electrostatic potential induced by the interfacial charge transfer, obtained by solving Poisson’s equation.(d) Calculated Bader charge transfer values for Sb and O atoms in the three phases.

## References


1. G. Kresse and J. Furthmüller, *Comput. Mater. Sci.*, 1996, **6**, 15-50.
2. G. Kresse and D. Joubert, *Phys. Rev. B*, 1999, **59**, 1758-1775.
3. P. E. Blöchl, *Phys. Rev. B*, 1994, **50**, 17953-17979.
4. S. Grimme, S. Ehrlich and L. Goerigk, *J. Comput. Chem.*, 2011, **32**, 1456-1465.